Image Segmentation by Oriented Image Foresting Transform with Geodesic Star Convexity

Lucy A.C. Mansilla and Paulo A.V. Miranda

Department of Computer Science, University of São Paulo (USP),
05508-090, São Paulo, SP, Brazil
{lucyacm,pmiranda}@vision.ime.usp.br

Abstract. Anatomical structures and tissues are often hard to be segmented in medical images due to their poorly defined boundaries, i.e., low contrast in relation to other nearby false boundaries. The specification of the boundary polarity and the usage of shape constraints can help to alleviate part of this problem. Recently, an Oriented Image Foresting Transform (OIFT) has been proposed. In this work, we discuss how to incorporate Gulshan's geodesic star convexity prior in the OIFT approach for interactive image segmentation, in order to simultaneously handle boundary polarity and shape constraints. This convexity constraint eliminates undesirable intricate shapes, improving the segmentation of objects with more regular shape. We include a theoretical proof of the optimality of the new algorithm in terms of a global maximum of an oriented energy function subject to the shape constraints, and show the obtained gains in accuracy using medical images of thoracic CT studies.

Keywords: graph search algorithms, image foresting transform, graph-cut segmentation, geodesic star convexity.

1 Introduction

Image segmentation, such as to extract an object from a background, is very useful for medical and biological image analysis. However, in order to guarantee reliable and accurate results, user supervision is still required in several segmentation tasks, such as the extraction of poorly defined structures in medical imaging, due to their intensity non-standardness among images, field inhomogeneity, noise, partial volume effects, and their interplay [1]. The high-level, application-domain-specific knowledge of the user is also often required in the digital matting of natural scenes, because of their heterogeneous nature [2]. These problems motivated the development of several methods for semi-automatic segmentation [3,4,5,6], aiming to minimize the user involvement and time required without compromising accuracy and precision.

One important class of interactive image segmentation comprises seed-based methods, which have been developed based on different theories, supposedly not related, leading to different frameworks, such as watershed [6], random

R. Wilson et al. (Eds.): CAIP 2013, Part I, LNCS 8047, pp. 572–579, 2013.

walks [7], fuzzy connectedness [8], graph cuts [4], distance cut [2], image foresting transform [9], and grow cut [10]. The study of the relations among different frameworks, including theoretical and empirical comparisons, has a vast literature [11,12,13,14]. These methods can also be adapted to automatic segmentation whenever the seeds can be automatically found [15].

In this paper, we pursue our previous work on *Oriented Image Foresting Transform* (OIFT) [16], which extends popular methods [9,8], by incorporating the boundary orientation (boundary polarity) to resolve between very similar nearby boundary segments by exploring directed weighted graphs. OIFT presents an excellent trade-off between time efficiency and accuracy, and is extensible to multidimensional images. In this work, we discuss how to incorporate Gulshan's geodesic star convexity (GSC) prior in the OIFT approach. This convexity constraint eliminates undesirable intricate shapes, improving the segmentation of objects with more regular shape. We include a theoretical proof of the optimality of the new algorithm in terms of a global maximum of an energy function subject to the shape constraints. The proposed method GSC-OIFT can simultaneously handle boundary polarity and shape constraints with improved accuracy for targeted image segmentation [17].

The next sections give a summary of the relevant previous work of the *Image Foresting Transform* [9] and OIFT [16]. The proposed extensions are presented in Section 5. In Section 6, we evaluate the methods, and state our conclusions.

2 Image Foresting Transform

An image can be interpreted as a weighted graph $G = (\mathcal{I}, \mathcal{A}, w)$ whose nodes are the image pixels in its image domain $\mathcal{I} \subset Z^n$, and whose arcs are the pixel pairs (s,t) in $\mathcal{A}$ (e.g., 4-neighborhood, or 8-neighborhood, in case of 2D images). The *adjacency relation* $\mathcal{A}$ is a binary relation on $\mathcal{I}$. We use $t \in \mathcal{A}(s)$ and $(s,t) \in \mathcal{A}$ to indicate that t is adjacent to s. Each arc $(s,t) \in \mathcal{A}$ has a fixed weight $w(s,t) \geq 0$. In this work, higher arc weights across the object's boundary should be considered, such as a dissimilarity measure between pixels s and t (e.g., $w(s,t) = |I(t) - I(s)|$ for a single channel image with values given by $I(t)$). The graph is undirected weighted if $w(s,t) = w(t,s)$ for all $(s,t) \in \mathcal{A}$, otherwise we have a directed weighted graph.

For a given image graph $G = (\mathcal{I}, \mathcal{A}, w)$, a path $\pi_t = \langle t_1, t_2, \ldots, t \rangle$ is a sequence of adjacent pixels with terminus at a pixel t. A path is *trivial* when $\pi_t = \langle t \rangle$. A path $\pi_t = \pi_s \cdot \langle s,t \rangle$ indicates the extension of a path π_s by an arc (s,t). A *predecessor map* is a function P that assigns to each pixel t in $\mathcal{I}$ either some other adjacent pixel in $\mathcal{I}$, or a distinctive marker *nil* not in $\mathcal{I}$ — in which case t is said to be a *root* of the map. A *spanning forest* is a predecessor map which contains no cycles — i.e., one which takes every pixel to *nil* in a finite number of iterations. For any pixel $t \in \mathcal{I}$, a spanning forest P defines a path π_t recursively as $\langle t \rangle$ if $P(t) = nil$, and $\pi_s \cdot \langle s,t \rangle$ if $P(t) = s \neq nil$.

A *connectivity function* computes a value $f(\pi_t)$ for any path π_t, usually based on arc weights. A path π_t is *optimum* if $f(\pi_t) \leq f(\tau_t)$ for any other

path τ_t in G. By taking to each pixel $t \in \mathcal{I}$ one optimum path with terminus t, we obtain the optimum-path value $V(t)$, which is uniquely defined by $V(t) = \min_{\forall \pi_t \text{ in } G}\{f(\pi_t)\}$. The *image foresting transform* (IFT) [9] takes an image graph $G = (\mathcal{I}, \mathcal{A}, w)$, and a path-value function f; and assigns one optimum path π_t to every pixel $t \in \mathcal{I}$ such that an *optimum-path forest* P is obtained — i.e., a spanning forest where all paths are optimum. However, f must be *smooth* [9], otherwise, the paths may not be optimum.

The cost of a trivial path $\pi_t = \langle t \rangle$ is usually given by a handicap value $H(t)$, while the connectivity functions for non-trivial paths follow a path-extension rule. For example:

$$f_{\max}(\pi_s \cdot \langle s,t \rangle) = \max\{f_{\max}(\pi_s), w(s,t)\} \tag{1}$$

$$f_{sum}(\pi_s \cdot \langle s,t \rangle) = f_{sum}(\pi_s) + \delta(s,t) \tag{2}$$

$$f_{euc}(\pi_s \cdot \langle s,t \rangle) = \|t - R(\pi_s)\|^2 \tag{3}$$

$$f_{w}(\pi_s \cdot \langle s,t \rangle) = w(s,t) \tag{4}$$

where $w(s,t) \geq 0$ is a fixed arc weight, $\delta(s,t) \geq 0$ is a dissimilarity measure, $R(\pi_t)$ is the origin/root of a path π_t, and f_w is a non-smooth function, which has important relations with the $f_{\max}$ smooth function [18,12].

We consider image segmentation from two seed sets, $\mathcal{S}_o$ and $\mathcal{S}_b$ ($\mathcal{S}_o \cap \mathcal{S}_b = \emptyset$), containing pixels selected inside and outside the object, respectively. The search for optimum paths (usually considering $f_{\max}$) is constrained to start in $\mathcal{S} = \mathcal{S}_o \cup \mathcal{S}_b$ (i.e., $H(t) = -1$ for all $t \in S$, and $H(t) = +\infty$ otherwise). The image is partitioned into two optimum-path forests — one rooted at the internal seeds, defining the object, and the other rooted at the external seeds, representing the background [18]. A label, $L(t) = 1$ for all $t \in \mathcal{S}_o$ and $L(t) = 0$ for all $t \in \mathcal{S}_b$, is propagated to all unlabeled pixels during the computation [9].

In the case of undirected weighted graphs, the connectivity functions $f_{\max}$ (under the conditions stated in [18]) and f_w give a global optimum segmentation according to an energy function of the cut boundary [13,14]. They maximize the graph-cut measure E defined by Equation 5 among all possible segmentation results satisfying the hard constraints (seeds).

$$E(L, G = (\mathcal{I}, \mathcal{A}, w)) = \min_{\forall (s,t) \in \mathcal{A} |\ L(s) \neq L(t)} w(s,t) \tag{5}$$

3 Oriented Image Foresting Transform (OIFT)

In the case of directed graphs, an important thing to note is that there are two different types of cut for each object boundary: an inner-cut boundary composed by edges that point toward object pixels $\mathcal{C}_i(L) = \{\forall (s,t) \in \mathcal{A} |\ L(s) = 0, L(t) = 1\}$, and an outer-cut boundary with edges from object to background pixels $\mathcal{C}_o(L) = \{\forall (s,t) \in \mathcal{A} |\ L(s) = 1, L(t) = 0\}$. Consequently, we have two different kinds of energy, $E_i(L,G)$ and $E_o(L,G)$:

$$E_i(L, G = (\mathcal{I}, \mathcal{A}, w)) = \min_{\forall (s,t) \in \mathcal{C}_i(L)} w(s,t) \tag{6}$$

$$E_o(L, G = (\mathcal{I}, \mathcal{A}, w)) = \min_{\forall (s,t) \in \mathcal{C}_o(L)} w(s,t) \tag{7}$$

As demonstrated in [16], the following non-smooth connectivity functions $f^{bkg}_{i,\max}$ and $f^{bkg}_{o,\max}$ in the IFT algorithm (which we denote as OIFT) lead to optimum cuts that maximize Eq. 6 and Eq. 7, respectively. The handicap values of $f^{bkg}_{i,\max}$ and $f^{bkg}_{o,\max}$ for trivial paths are defined as before (i.e., $H(t) = -1$ for all $t \in S$, and $H(t) = +\infty$ otherwise). The undirected weights $w(s,t)$ are converted to directed arcs by multiplying them by an orientation factor $(1+\alpha)$ if $I(s) > I(t)$, and by $(1-\alpha)$ otherwise (e.g., $\alpha = 0.5$).

$$f^{bkg}_{i,\max}(\pi_s \cdot \langle s,t \rangle) = \begin{cases} \max\{f^{bkg}_{i,\max}(\pi_s), 2 \times w(t,s) + 1\} & \text{if } R(\pi_s) \in \mathcal{S}_o \\ \max\{f^{bkg}_{i,\max}(\pi_s), 2 \times w(s,t)\} & \text{if } R(\pi_s) \in \mathcal{S}_b \end{cases} \quad (8)$$

$$f^{bkg}_{o,\max}(\pi_s \cdot \langle s,t \rangle) = \begin{cases} \max\{f^{bkg}_{o,\max}(\pi_s), 2 \times w(s,t) + 1\} & \text{if } R(\pi_s) \in \mathcal{S}_o \\ \max\{f^{bkg}_{o,\max}(\pi_s), 2 \times w(t,s)\} & \text{if } R(\pi_s) \in \mathcal{S}_b \end{cases} \quad (9)$$

4 Geodesic Star Convexity (GSC)

A point p is said to be visible to c via a set $\mathcal{O}$ if the line segment joining p to c lies in the set $\mathcal{O}$. An object $\mathcal{O}$ is star-convex with respect to center c, if every point $p \in \mathcal{O}$ is visible to c via $\mathcal{O}$ [19]. It is also possible to define a discrete version of this constraint directly in the image domain, by considering a shortest path in the image graph, returned by the IFT (e.g., using f_{euc}, 8-connected adjacency, $H(c) = 0$, and $H(t) = +\infty$ for all $t \neq c$), as the line segment.

In the case of multiple stars, a computationally tractable definition, was proposed in [20]. The previous notion of the line segment (shortest path) joining the single star center c to p, is extended to a line segment joining the set of star centers $C = \{c_1, c_2, \ldots, c_n\}$ to p, which is taken as the shortest path between the point p and set C. In interactive segmentation, the set of star centers is usually taken to coincide with the internal seeds (i.e., $C = \mathcal{S}_o$), and, in the discrete version, the line segments form a spanning forest rooted at the internal seeds, where each line segment corresponds to a path in the graph.

In [20], the authors proposed the usage of a different notion of star convexity with shortest path from Euclidean to geodesic (f_{sum}). We use $H(t) = -1$ for all $t \in \mathcal{S}_o$ ($H(t) = +\infty$ otherwise), and $\delta(s,t) = [w(s,t)+1]^\beta - 1 + \|t-s\|$ in the path-extension rule for f_{sum}, where $\|t-s\|$ is the Euclidean distance between pixels s and t, and β controls the forest topology in the returned predecessor map, which we will denote by P_{sum}. For lower values of β ($\beta \approx 0.0$), $\delta(s,t)$ approaches $\|t-s\|$, and it imposes more star regularization to the object's boundary. For higher values, $[w(s,t)+1]^\beta$ dominates the expression, allowing a better fit to the curved protrusions and indentations of the boundary.

5 OIFT with Geodesic Star Convexity (GSC-OIFT)

An object $\mathcal{O}$ is geodesic star convex (GSC) with respect to a set of centers C, if every point $p \in \mathcal{O}$ is visible to C via $\mathcal{O}$ (i.e., the shortest path joining p to

C in P_{sum} lies in the set $\mathcal{O}$). In this work, we want to constrain the search for optimum results, that maximize the graph-cut measures $E_i(L,G)$ (Eq. 6) and $E_o(L,G)$ (Eq. 7), only to segmentations that satisfy the geodesic star convexity constraint.

First, we compute the optimum forest P_{sum} for f_{sum} by the regular IFT algorithm, using only $\mathcal{S}_o$ as seeds, for the given directed graph $G = (\mathcal{I}, \mathcal{A}, w)$. Let's consider the following two sets of arcs $\xi^i_{P_{sum}} = \{\forall (s,t) \in \mathcal{A} |\ s = P_{sum}(t)\}$ and $\xi^o_{P_{sum}} = \{\forall (s,t) \in \mathcal{A} |\ t = P_{sum}(s)\}$. We have the following Lemma 1:

Lemma 1. *For a given segmentation L, we have $\mathcal{C}_o(L) \cap \xi^o_{P_{sum}} \neq \emptyset$, if and only if there is a violation of the geodesic star convexity constraint. We have $\mathcal{C}_i(L) \cap \xi^i_{P_{sum}} \neq \emptyset$, if and only if there is a violation of the geodesic star convexity constraint.*

Proof. We will demonstrate it for $\mathcal{C}_o(L) \cap \xi^o_{P_{sum}} \neq \emptyset$, but the demonstration for $\mathcal{C}_i(L) \cap \xi^i_{P_{sum}} \neq \emptyset$ is essentially identical. By definition, a violation of geodesic star convexity constraint with respect to a set of centers $C = \mathcal{S}_o$, will be given if there exists a point $p \in \mathcal{O} = \{\forall t | L(t) = 1\}$ that is not visible to C via $\mathcal{O}$ (i.e., there is a pixel r in the shortest path joining p to C in P_{sum}, and $r \notin \mathcal{O}$).

By the definitions of $\xi^o_{P_{sum}}$ and $\mathcal{C}_o(L)$, we have $\mathcal{C}_o(L) \cap \xi^o_{P_{sum}} = \{\forall (s,t) \in A | L(s) = 1, L(t) = 0$ *and* $t = P_{sum}(s)\}$. For any edge $(s,t) \in \mathcal{C}_o \cap \xi^o_{P_{sum}}$ we have $t = P_{sum}(s)$, which means that there exists a shortest path $\pi_s = \pi_t \cdot \langle t, s \rangle$ in P_{sum} rooted at the internal seeds S_o (i.e., line segment between s and S_o). But $(s,t) \in \mathcal{C}_o(L)$ implies that $L(t) = 0$ (i.e., $t \notin \mathcal{O}$), and hence s is not visible to $\mathcal{S}_o$ through $\pi_s = \pi_t \cdot \langle t, s \rangle$ in P_{sum}. Thus, $\mathcal{C}_o \cap \xi^o_{P_{sum}} \neq \emptyset$ implies in a violation of the geodesic star convexity constraint.

On the other hand, if we have a violation of the geodesic star convexity constraint, it means that $\exists s \in \mathcal{O}$ (i.e., $L(s) = 1$), which is not visible to S_o via the shortest path π_s in P_{sum}, so that there is a pixel $p_i \notin \mathcal{O}$ in $\pi_s = \langle p_1, \ldots, p_i, \ldots, p_n = s \rangle$, with $P_{sum}(p_{i+1}) = p_i$ and $p_{i+1} \in \mathcal{O}$. Hence, $(p_{i+1}, p_i) \in \mathcal{C}_o \cap \xi^o_{P_{sum}}$, which implies that $\mathcal{C}_o \cap \xi^o_{P_{sum}} \neq \emptyset$.

Therefore, we have $\mathcal{C}_o \cap \xi^o_{P_{sum}} \neq \emptyset$, if and only if there is a violation of the geodesic star convexity constraint.

Theorem 1 (Inner/outer-cut boundary optimality). *For a given image graph $G = (\mathcal{I}, \mathcal{A}, w)$, consider a modified weighted graph $G' = (\mathcal{I}, \mathcal{A}, w')$, with weights $w'(s,t) = -\infty$ for all $(s,t) \in \xi^o_{P_{sum}}$, and $w'(s,t) = w(s,t)$ otherwise. For two given sets of seeds $\mathcal{S}_o$ and $\mathcal{S}_b$, the segmentation computed over G' by the IFT algorithm for function $f^{bkg}_{o,\max}$ defines an optimum cut in the original graph G, that maximizes $E_o(L,G)$ among all possible segmentation results satisfying the shape constraints by the geodesic star convexity, and the seed constraints.*

Similarly, the segmentation computed by the IFT algorithm for function $f^{bkg}_{i,\max}$, over a modified graph $G' = (\mathcal{I}, \mathcal{A}, w')$; with weights $w'(s,t) = -\infty$ for all $(s,t) \in \xi^i_{P_{sum}}$, and $w'(s,t) = w(s,t)$ otherwise; defines an optimum cut in the original graph G, that maximizes $E_i(L,G)$ among all possible segmentation results satisfying the shape constraints by the geodesic star convexity, and the seed constraints.

Proof. We will prove the theorem in the case of function $f^{bkg}_{o,\max}$ the other case having essentially identical proof. Since we assign the worst weight to all arcs $(s,t) \in \xi^o_{P_{sum}}$ in G' (i.e., $w'(s,t) = -\infty$), any segmentation $\tilde{L}$ with $\mathcal{C}_o(\tilde{L}) \cap \xi^o_{P_{sum}} \neq \emptyset$ will receive the worst energy value ($E_o(\tilde{L}, G') = -\infty$) [1]. From the Theorem in [16], we know that the IFT with $f^{bkg}_{o,\max}$ over G' maximizes the energy $E_o(L, G')$ in the graph G', consequently, it will naturally avoid in its outer-cut boundary any edge from $\xi^o_{P_{sum}}$. Since, there is always a solution that does not violate the GSC constraint (e.g., we could take $\mathcal{O} = \mathcal{S}_o$), and from Lemma 1, we have that the computed solution cannot violate the GSC constraint.

Since $w(s,t) \geq 0, \forall (s,t) \in \mathcal{A}$, and from Lemma 1, we have that any candidate segmentation $\ddot{L}$ satisfying the GSC constraint must have $E_o(\ddot{L}, G') \geq 0$. Moreover, since its weights for the arcs in $\mathcal{C}_o(\ddot{L})$ were not changed in G', we also have that $E_o(\ddot{L}, G') = E_o(\ddot{L}, G)$. Hence, all results satisfying the GSC constraint were considered in the optimization, and therefore Theorem 1 holds, as we wanted to prove.

6 Experiments and Conclusions

We conducted quantitative experiments, using a total of 40 image slices of 10 thoracic CT studies to segment the liver. All methods, including the power watershed algorithm ($\text{PW}_{q=2}$) [14], were assessed for accuracy employing the mean performance curve (Dice coefficient) and ground truth data obtained from an expert of the radiology department at the University of Pennsylvania.

Figure 1a shows the mean accuracy curves for all the images assuming different seed sets obtained by eroding and dilating the ground truth. The undirected arc weights were computed as $w(s,t) = |I(t) - I(s)|$. For the directed weighted graphs we considered $\alpha = 0.5$, and we used $\beta = 0.0$. For higher values of β, GSC-OIFT imposes less shape constraints, so that the accuracy tends to decrease (Fig. 1b-d). Figure 2 shows some results in the case of user-selected markers for the liver, and Figure 3 shows one example in 3D.

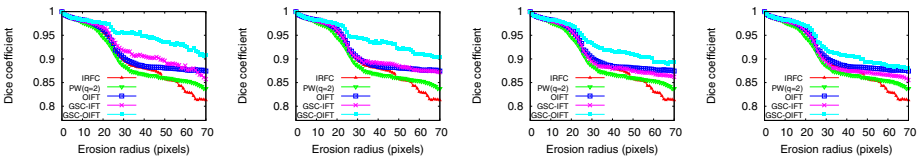

(a) (b) (c) (d)

Fig. 1. (a) The mean accuracy curves of all methods for the liver segmentation for various values of β: (a) $\beta = 0.0$, (b) $\beta = 0.2$, (c) $\beta = 0.5$, and (d) $\beta = 0.7$

[1] The GSC restrictions are embedded directly into the graph G'.

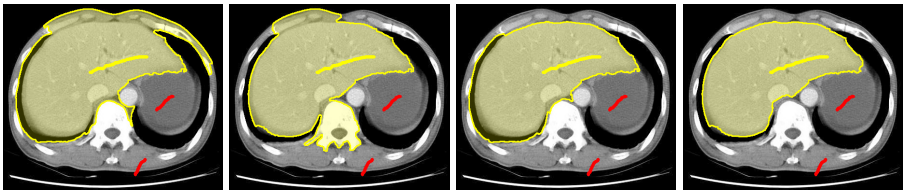

(a) (b) (c) (d)

Fig. 2. Results for user-selected markers: (a) IRFC (IFT with $f_{\max}$), (b) OIFT ($f^{bkg}_{o,\max}$ with $\alpha = 0.5$), (c) GSC-IFT ($\beta = 0.7$, $\alpha = 0.0$), and (d) GSC-OIFT ($\beta = 0.7$, $\alpha = 0.5$)

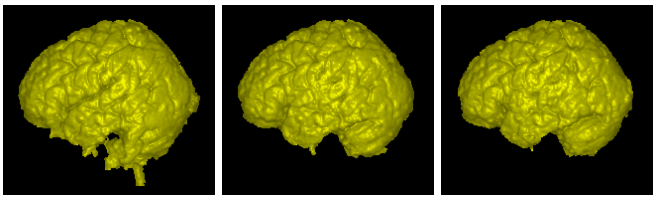

(a) (b) (c)

Fig. 3. Example of 3D skull stripping in MRI: (a) IRFC (IFT with $f_{\max}$), (b) GSC-IFT ($\beta = 0.3$, $\alpha = 0.0$), and (c) GSC-OIFT ($\beta = 0.3$, $\alpha = 0.5$), for the same user-selected markers

In conclusion, we developed extensions to the OIFT algorithm [16], by incorporating the geodesic star convexity constraint in its formulation. The results were proved to be optimum according to an energy functional of the cut boundary, and were shown to improve the accuracy in practice. GSC-OIFT only requires twice the computational time of a conventional IFT. As future work, we intend to combine it with statistical models for automatic segmentation.

Acknowledgment. The authors thank FAPESP (2012/06911-2), CNPq (305381/2012-1), and CAPES for the financial support, and Dr. J. K. Udupa (MIPG-UPENN) for the images.

References

1. Madabhushi, A., Udupa, J.: Interplay between intensity standardization and inhomogeneity correction in MR image processing. IEEE Transactions on Medical Imaging 24(5), 561–576 (2005)
2. Bai, X., Sapiro, G.: Distance cut: Interactive segmentation and matting of images and videos. In: Proc. of the IEEE Intl. Conf. on Image Processing, vol. 2, pp. II-249–II-252 (2007)
3. Falcão, A., Udupa, J., Samarasekera, S., Sharma, S., Hirsch, B., Lotufo, R.: User-steered image segmentation paradigms: Live-wire and live-lane. Graphical Models and Image Processing 60(4), 233–260 (1998)

4. Boykov, Y., Funka-Lea, G.: Graph cuts and efficient N-D image segmentation. Intl. Journal of Computer Vision 70(2), 109–131 (2006)
5. Kass, M., Witkin, A., Terzopoulos, D.: Snakes: Active contour models. Intl. Journal of Computer Vision 1, 321–331 (1987)
6. Cousty, J., Bertrand, G., Najman, L., Couprie, M.: Watershed cuts: Thinnings, shortest path forests, and topological watersheds. Trans. on Pattern Analysis and Machine Intelligence 32, 925–939 (2010)
7. Grady, L.: Random walks for image segmentation. IEEE Trans. Pattern Anaysis and Machine Intelligence 28(11), 1768–1783 (2006)
8. Ciesielski, K., Udupa, J., Saha, P., Zhuge, Y.: Iterative relative fuzzy connectedness for multiple objects with multiple seeds. Computer Vision and Image Understanding 107(3), 160–182 (2007)
9. Falcão, A., Stolfi, J., Lotufo, R.: The image foresting transform: Theory, algorithms, and applications. IEEE Transactions on Pattern Analysis and Machine Intelligence 26(1), 19–29 (2004)
10. Vezhnevets, V., Konouchine, V.: "growcut" - interactive multi-label N-D image segmentation by cellular automata. In: Proc. Graphicon., pp. 150–156 (2005)
11. Sinop, A., Grady, L.: A seeded image segmentation framework unifying graph cuts and random walker which yields a new algorithm. In: Proc. of the 11th International Conference on Computer Vision, ICCV, pp. 1–8. IEEE (2007)
12. Miranda, P., Falcão, A.: Elucidating the relations among seeded image segmentation methods and their possible extensions. In: XXIV Conference on Graphics, Patterns and Images, Maceió, AL (August 2011)
13. Ciesielski, K., Udupa, J., Falcão, A., Miranda, P.: Fuzzy connectedness image segmentation in graph cut formulation: A linear-time algorithm and a comparative analysis. Journal of Mathematical Imaging and Vision (2012)
14. Couprie, C., Grady, L., Najman, L., Talbot, H.: Power watersheds: A unifying graph-based optimization framework. Trans. on Pattern Anal. and Machine Intelligence 99 (2010)
15. Miranda, P., Falcão, A., Udupa, J.: Cloud bank: A multiple clouds model and its use in MR brain image segmentation. In: Proc. of the IEEE Intl. Symp. on Biomedical Imaging, Boston, MA, pp. 506–509 (2009)
16. Miranda, P., Mansilla, L.: Oriented image foresting transform segmentation by seed competition. IEEE Transactions on Image Processing (accepted, to appear, 2013)
17. Lézoray, O., Grady, L.: Image Processing and Analysis with Graphs: Theory and Practice. CRC Press, California (2012)
18. Miranda, P., Falcão, A.: Links between image segmentation based on optimum-path forest and minimum cut in graph. Journal of Mathematical Imaging and Vision 35(2), 128–142 (2009)
19. Veksler, O.: Star shape prior for graph-cut image segmentation. In: Forsyth, D., Torr, P., Zisserman, A. (eds.) ECCV 2008, Part III. LNCS, vol. 5304, pp. 454–467. Springer, Heidelberg (2008)
20. Gulshan, V., Rother, C., Criminisi, A., Blake, A., Zisserman, A.: Geodesic star convexity for interactive image segmentation. In: Proc. of Computer Vision and Pattern Recognition, pp. 3129–3136 (2010)